ResearchGate

See discussions, stats, and author profiles for this publication at: https://www.researchgate.net/publication/226359641

Polymer Chains and Networks in Narrow Slits

CHAPTER · JANUARY 1970

DOI: 10.1007/1-4020-2760-5_12

READS

10

3 AUTHORS:

Giuseppe Allegra

Politecnico di Milano

175 PUBLICATIONS **2,888** CITATIONS

SEE PROFILE

Guido Raos

Politecnico di Milano

92 PUBLICATIONS **1,736** CITATIONS

SEE PROFILE

Carlo Manassero

University of Milan

23 PUBLICATIONS **176** CITATIONS

SEE PROFILE

All in-text references underlined in blue are linked to publications on ResearchGate, letting you access and read them immediately.

Available from: Guido Raos
Retrieved on: 16 January 2016

POLYMER CHAINS AND NETWORKS IN NARROW SLITS

Highlights of recent results

Giuseppe Allegra, Guido Raos and Carlo Manassero
Dipartimento di Chimica, Materiali e Ingegneria Chimica "G. Natta"
Via L. Mancinelli 7, 20131 Milano, Italy
giuseppe.allegra@polimi.it

Abstract We review some recent results obtained by our group, on the general subject of polymers confined within narrow slits. First, we present a derivation of the free energy of compression of two- and three-dimensional networks between parallel walls. Then, we consider the problem of the adhesion between two parallel surfaces, produced by an ensemble of chains forming irreversible and randomly distributed bonds with the walls. We evaluate the free energy change and the elastic moduli of the polymer layer, corresponding to both tangential (shear) and normal (elongation and compression) deformations. Both calculations adopt different variants the phantom chain model, whereby polymer-polymer interactions are neglected.

Introduction

A better understanding the static and dynamical properties of polymers confined within narrow slits would have important implications for a number of seemingly unrelated phenomena. These include polymer-mediated adhesion and lubrication, the elasticity and failure of polymer-based composites or particle-filled rubbers, size-exclusion chromatography, colloid aggregation and stabilization, and nanofabrication of materials[1–4]. In view of the experimental difficulties and the number of variables affecting the possible outcome of an experiment, some of these phenonema have been traditionally considered as "engineering" subjects, with little room for "basic science". However, the situation has changed considerably in recent years. In particular, the development of the surface force apparatus has represented a major step forward on the experimental front[1]. Different variants of the instrument are now operative

P. Pasini et al. (eds.), Computer Simulations of Liquid Crystals and Polymers, 249-268.
© 2005 *Kluwer Academic Publishers. Printed in the Netherlands.*

in several laboratories, allowing the accurate measurement of both normal (compression and extension) and tangential (shear) forces, under both static and dynamic consitions, for confined polymeric films and brushes at wall-to-wall distances of the order of a few nanometers. See for example refs.[5–11] for further reviews and recent applications. These have often highlighted dramatic modifications in the polymer properties, which may turn for example from rubbery to solid-like on going from the bulk to the confined state.

The present article summarizes two recent theoretical contributions by our group, respectively addressing the elastic properties of compressed polymer networks[12] and of an adhesive polymer layer bridging two parallel surfaces[13]. Hopefully, the general methods and the specific results described here will provide a useful complement to scaling arguments [14, 15], which form the backbone of much polymer physics and have been largely invoked in the interpretation of the experimental results. In both cases, we adopt the phantom chain model, whereby chain-chain interactions (excluded-volume and entanglements) are neglected. The chains are thus expected to adopt random-walk conformations, as in polymer melts, dry cross-linked rubbers and Θ solutions[14, 15]. Within this model, the system's elasticity is entirely entropic in nature and arises from changes in the large-scale conformational state of the chains. If desired, a first-order estimate of enthalpic contributions to the system's elasticity may be recovered separately by a mean-field Flory-Huggins free energy term.

Before we go into greater detail, and considering general scope and purpose of the present volume, it seems appropriate to discuss briefly computer simulation methods. As in every other field of contemporary chemistry and physics, their importance has been growing steadily and is bound to increase even further in the future. Here we simply mention some recent publications, with the aim to provide some entry points to the literature and give a flavour for the variety of approaches which have been successfully adopted. Yoon, Vacatello and Smith[16] have given a useful summary of the situation up to 1995, with a special emphasis on their Monte Carlo simulations on united-atom models of confined polymer melts. More recently, Vacatello has addressed the effect of chain stiffness on packing and orientational order at the polymer-wall interface[17]. Binder and coworkers have applied on- and off-lattice Monte Carlo simulations to a number of problems, including for example the scaling properties of confined polymer solutions[18] or the glass transition of polymer melts in narrow slits[19]. The former problem has also been investigated by mesoscale field-theoretic simulations[20]. Ref. [21] describes a representative application of the molecular dynamics

method to the equilibrim properties of confined polymer melts. Simulations have also acted as a benchmark for integral equation and density functional theories of polymeric liquids at solid surfaces[22]. Finally, the molecular and Brownian dynamics methods have been applied to steady-state non-equilibrium situations, such as the sliding of interpenetating polymer brushes under shear[11, 23]. All the studies mentioned above adopt some kind of coarse-grained description of system. The simulation of adhesion and friction between atomistically detailed models of self-assembled alkylsilane monolayers[24] may be cited as an interesting exception.

The rest of the paper consists of two separate Sections, respectively on the compression of polymer networks and on polymer-mediated adhesion. The two may be read independently of each other. We sketch the mathematical derivations, which are given more fully in refs.[12, 13], and try to emphasize the most significant physical results.

1. Compressed polymer networks

1.1 A Gaussian chain in a harmonic potential

Assuming that the confining walls are perpendicular to the x axis and are located at $x = \pm L/2$, we introduce a harmonic potential of the form:

$$\frac{V(x)}{k_B T} = \frac{1}{2} H \left(\frac{x}{l} \right)^2 , \tag{1}$$

where $k_B T$ is the thermal energy and l is the root-mean-square (r.m.s) length of the polymer segments. These are the natural units in the present problem, and they will be omitted in the following equations in order to simplify the notation. Both the compression energy (E_H) and the mean-square (m.s) distance of the network elements from the center of the slab (Δ_H^2) may be derived from the partition function Z_H. An increase of H has the obvious effect of increasing E_H and diminishing Δ_H^2. The square root of the latter may be identified with the slab width L (to within a factor of the order of unity). We shall then use H as a "driving parameter" in order to establish the relationship between compression energy and slab width.

We consider a long Gaussian chain made up of $n+1$ beads connected by n harmonic springs, each of elastic constant $\kappa = 3$ (this is actually $\kappa = 3k_B T/l^2$, but takes the simpler form because of our choice of the energy and length units). Its Hamiltonian is:

$$\mathcal{H}\{x_i\} = \frac{3}{2} \sum_{i=1}^{n} (x_i - x_{i-1})^2 + \frac{1}{2} H \sum_{i=0}^{n} x_i^2 = \tag{2}$$

$$= \frac{1}{2}\mathbf{x}(3\mathbf{R} + H\mathbf{I})\mathbf{x}^T \tag{3}$$

where $\mathbf{x}$ is a row vector containing the bead coordinates, $\mathbf{I}$ is the $(n+1) \times (n+1)$ unit matrix and $\mathbf{R}$ is the Rouse matrix for an open linear chain[29, 30]:

$$\mathbf{R} = \begin{bmatrix} 1 & -1 & 0 & 0 & ... & 0 \\ -1 & 2 & -1 & 0 & ... & 0 \\ 0 & -1 & 2 & -1 & ... & 0 \\ ... & ... & ... & ... & ... & ... \\ 0 & 0 & ... & 0 & -1 & 1 \end{bmatrix} . \tag{4}$$

The first term in Eq.(2) accounts for the chain connectivity, the second one for the confining potential. Note that we consider explicitly only one spatial dimension (x) and neglect the other two (y and z). The reason is that these components give rise to additional terms of the Hamiltonian which, however, are irrelevant since they are independent of the external field $V(x)$. In other words, the statistics of the chain along y and z are not affected by confinement along x (this would not be true for a more complex model with excluded-volume interactions among the beads, where "squeezing" along x is expected to produce an expansion in the orthogonal directions).

The partition function of an *unconstrained* chain, where all beads are free to fluctuate under the quadratic field, is:

$$Z_H = \int \cdots \int \prod_{i=0}^{n} dx_i \exp\left[-\mathcal{H}\{x_i\}\right] . \tag{5}$$

This may be evaluated by changing integration variables according to the orthogonal transformation which diagonalizes $(3\mathbf{R} + H\mathbf{I})$ and using the standard formulae for Gaussian integrals:

$$Z_H = \left[\prod_{p=0}^{n} \frac{2\pi}{3\lambda_p + H}\right]^{1/2} . \tag{6}$$

The λ_p's are the eigenvalues of $\mathbf{R}$:

$$\lambda_p = 2\left(1 - \cos\frac{p\pi}{n+1}\right) . \tag{7}$$

The m.s distance of the beads from the median plane is obtained by differentiation of the partition function:

$$\Delta_H^2 = \frac{1}{n+1} \frac{\int \cdots \int \prod_i dx_i \left[\sum_j x_j^2\right] \exp\left[-\mathcal{H}\{x_i\}\right]}{\int \cdots \int \prod_i dx_i \exp\left[-\mathcal{H}\{x_i\}\right]}$$

$$= -\frac{2}{n+1}\frac{\partial \ln Z_H}{\partial H}. \tag{8}$$

In the large-n limit, this may be approximated as:

$$\Delta_H^2 \simeq \frac{1}{n}\sum_{p=0}^{\infty}\left[H + 3\frac{\pi^2 p^2}{n^2}\right]^{-1} = \frac{n}{12\sigma}\left[\coth 2\sigma + \frac{1}{2\sigma}\right], \tag{9}$$

where we have introduced the reduced variable σ:

$$\sigma^2 = \frac{n^2 H}{12}. \tag{10}$$

To a good approximation, Δ_H^2 may be identified with the m.s distance of the beads from the center-of-mass of the chain. This is actually the chain's m.s radius of gyration along x (S_x^2). The two quantities are related by:

$$\Delta_H^2 = S_x^2 + \delta_x^2 \tag{11}$$

where δ_x^2 is the m.s fluctuation of the center-of-mass from the middle of the slab. The latter may be safely neglected for a very long chain under a sufficiently strong confining potential, when $\sigma \gg 1$ or $n \gg 1/\sqrt{H}$. The reason is that a fluctuation of the center-of-mass off the median produces a minor entropic gain, which however has to be balanced against a large increase in potential energy.

The case of a *constrained* chain, with the two end beads fixed at coordinates X_A and X_B, will be useful for the following treatment of networks. Its partition function is now defined to be:

$$Z_H(X_A, X_B) = \int \cdots \int \prod_{i=0}^{n} dx_i \exp\left[-\mathcal{H}\{x_i\}\right] \delta(x_0 - X_A)\delta(x_n - X_B). \tag{12}$$

Note that we use similar symbols for the unconstrained and constrained partition functions. The dependence of the latter on the coordinates of the fixed beads will always be explicitly indicated, thus allowing the reader to distinguish between the two. The two δ functions are conveniently represented by the Fourier integrals:

$$\delta(x - X) = \frac{1}{2\pi}\int_{-\infty}^{+\infty} \exp\left\{i\omega(x - X)\right\} d\omega. \tag{13}$$

After some algebra, the final result may be cast in the form:

$$Z_H(X_A, X_B) = \zeta_H \exp\left[-\frac{B_H}{2}(X_A^2 + X_B^2) - \frac{C_H}{2}(X_A - X_B)^2\right], \tag{14}$$

where, in the large-n limit:

$$\begin{aligned} \zeta_H &= Z_H \frac{12\pi\sigma}{n}, \\ B_H &= \frac{6\sigma \tanh\sigma}{n}, \\ C_H &= \frac{3\sigma\,(\coth\sigma - \tanh\sigma)}{n}. \end{aligned} \tag{15}$$

Eq.(14) has a physically appealing interpretation. After integration over the internal bead coordinates, the partition function for the constrained chain is formally identical to the statistical weight of a dumbbell (two beads connected by a spring) in an external harmonic potential. However, both the "external potential" and the "spring" terms B_H and C_H depend on the confining potential through σ. In the limit of a vanishing field, we recover the usual result for a Gaussian chain of n links ($B_H \to 0$ and $C_H \to 3/n$). Interestingly, C_H is a decreasing function of σ, so that the effective spring becomes looser as the confining potential becomes stronger. This suggests interesting effects upon the spectrum of relaxation times of the chain.

1.2 The two-dimensional network

Let us consider a regular network of chains with square connectivity. Topologically, it has a dimensionality of two. All the chains comprise n springs, $n-1$ internal beads and two terminal ones. The latter represent the junctions and are shared with the adjacent chains. Each junction is labelled with two integer indexes, j running from 1 to J and k from 1 to K ($J, K \gg 1$). Letting $X_{j,k}$ be the x coordinate of a junction, the statistical weight of the network with fixed cross-link coordinates is

$$\mathcal{Z}_H\{X_{j,k}\} = \left[\prod_{j=1}^{J}\prod_{k=1}^{K} Z_H(X_{j,k}, X_{j+1,k})\right] \times \left[\prod_{j=1}^{J}\prod_{k=1}^{K} Z_H(X_{j,k}, X_{j,k+1})\right]. \tag{16}$$

The statistical weights $Z_H(X_{i,j}, X_{k,l})$ of the individual chains are given by Eq.(14). It is convenient to assume periodic boundary conditions along both topological directions, so that

$$X_{1,k} = X_{J+1,k}, \qquad X_{j,1} = X_{j,K+1} \qquad (\forall\, j,k). \tag{17}$$

The partition function of the unconstrained network is obtained from Eq.(16) by integration over the coordinates of the cross-links:

$$\begin{aligned} \mathcal{Z}_H &= \int \cdots \int \prod_{j=1}^{J} \prod_{k=1}^{K} dX_{j,k} \mathcal{Z}_H \{X_{j,k}\} \qquad (18) \\ &= (\zeta_H)^{2JK} \int \cdots \int \prod_{j=1}^{J} \prod_{k=1}^{K} dX_{j,k} \exp\left[-\frac{C_H}{2} \mathbf{X}\,\mathbf{U}\,\mathbf{X}^T\right], \end{aligned}$$

where $\mathbf{X}$ is a row vector containing the cross-link coordinates

$$\mathbf{X} = [X_{1,1} ... X_{J,1} ..... X_{1,K} ... X_{K,K}],$$

and $\mathbf{U}$ is a block-cyclic matrix with $K \times K$ square blocks

$$\mathbf{U} = \begin{bmatrix} \mathbf{\Sigma} & -\mathbf{I} & \mathbf{0} & ... & -\mathbf{I} \\ -\mathbf{I} & \mathbf{\Sigma} & -\mathbf{I} & ... & \mathbf{0} \\ \mathbf{0} & -\mathbf{I} & \mathbf{\Sigma} & ... & \mathbf{0} \\ ... & ... & ... & ... & ... \\ -\mathbf{I} & \mathbf{0} & ... & -\mathbf{I} & \mathbf{\Sigma} \end{bmatrix}. \qquad (19)$$

Each block of $\mathbf{U}$ is a $J \times J$ matrix, $\mathbf{I}$ being the indentity and

$$\mathbf{\Sigma} = \begin{bmatrix} 4\cosh 2\sigma & -1 & 0 & ... & -1 \\ -1 & 4\cosh 2\sigma & -1 & ... & 0 \\ 0 & -1 & 4\cosh 2\sigma & ... & 0 \\ ... & ... & ... & ... & ... \\ -1 & 0 & ... & -1 & 4\cosh 2\sigma \end{bmatrix}. \qquad (20)$$

Integration of Eq.(18) is carried out in analogy with single-chain case of Eq.(6):

$$\mathcal{Z}_H = (\zeta_H)^{2JK} \left[\prod_{u=1}^{J} \prod_{v=1}^{K} \frac{2\pi}{C_H \lambda_{u,v}}\right]^{1/2}. \qquad (21)$$

All that is required are the eigenvalues of $\mathbf{U}$ ($\lambda_{u,v}$, for $u = 1, ..., J$ and $v = 1, ..., K$). The cyclic nature of $\mathbf{U}$ and of its $\mathbf{\Sigma}$ blocks allows these to be obtained in closed analytical form:

$$\lambda_{u,v} = 4\cosh 2\sigma - 2\cos\frac{2\pi u}{J} - 2\cos\frac{2\pi v}{K}. \qquad (22)$$

Again, the m.s size of the network may be obtained from the derivative of $\ln Z$ [see Eq.(8)]:

$$\Delta_H^2 = -\frac{1}{nJK}\frac{\partial \ln \mathcal{Z}_H}{\partial H} = -\frac{1}{nJK}\frac{\partial \ln \mathcal{Z}_H}{\partial \sigma}\frac{d\sigma}{dH} \qquad (23)$$

The final result is:

$$\frac{\Delta_H^2}{n} = \frac{1}{48\sigma}\left[2\coth(2\sigma) - \frac{1}{\sigma} + \frac{4\tanh 2\sigma}{\pi}\mathbf{K}\left(\frac{1}{\cosh 2\sigma}\right)\right], \qquad (24)$$

where $\mathbf{K}$ is the complete elliptic integral of the first kind:

$$\mathbf{K}(q) = \int_0^1 \frac{dx}{\sqrt{(1-x^2)(1-q^2x^2)}} \qquad (q < 1).$$

The energy of compression E_H is given by

$$E_H = \left\langle \sum_i \frac{1}{2} H x_i^2 \right\rangle = \frac{1}{2}\left[2nJK\right] H \left\langle \Delta_H^2 \right\rangle. \qquad (25)$$

Remembering from Eq.(10) that $H = 12\sigma^2/n^2$, the energy *per chain* is then:

$$\mathcal{E}_H = \frac{E_H}{2JK} = 6\sigma^2 \frac{\langle \Delta_H^2 \rangle}{n}. \qquad (26)$$

1.3 Numerical results

Eqs.(24) and (26) are the main results of the previous section on two-dimensional networks. The m.s distance of the network elements from the minimum of the confining potential (proportional to the square of the slab width L^2) and the network energy per chain are expressed as a function of a compression parameter σ. The latter may be eliminated graphically, by driving it from a very small up to a very large value, and plotting $\mathcal{E}_H$ and Δ_H^2/n against each other. The result is given in Figure 1, alongside analogous plots for:

- a one-dimensional "network", made up of several chains connected head-to-tail to form a very large ring
- a three-dimensional network with cubic topology
- some intermediate cases, constructed by superposition of a finite number (2, 4 or 8) of two-dimensional layers, giving a three-dimensional network with finite thickness along one topological direction.

Mathematical details for these additional cases may be found in ref.[12].

Figure 1 demonstrates a very similar behaviour of the one-, two- and three-dimensional networks at strong compressions. When the external field is strong to the point of producing a compression of the individual strands, their topological connectivity becomes irrelevant. On the other

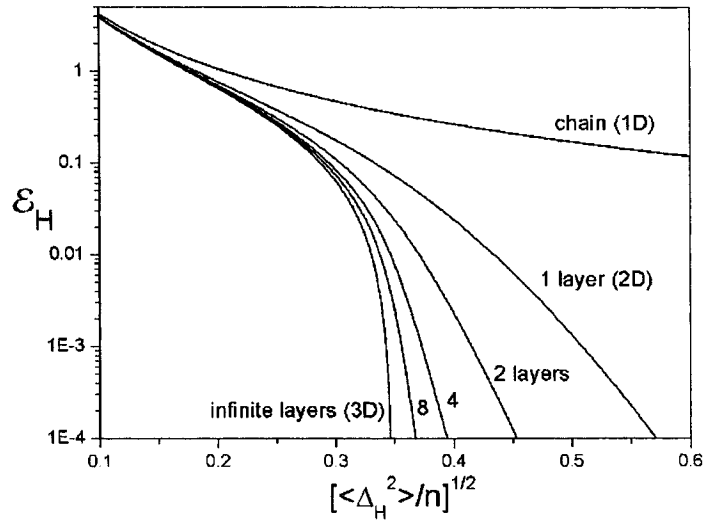

Figure 1. Reduced free energy per chain $\mathcal{E}_H$ vs. the reduced r.m.s distance of the beads from the slab center $\sqrt{\langle \Delta_x^2 \rangle / n}$ ($\simeq$ reduced slab width), for the one-, two- and three-dimensional networks.

hand, significant differences are observed under weak compression. In the limit of a vanishingly small applied field, Eq. (24) gives

$$\Delta_H^2 \simeq S_x^2 = n\,[a - b \ln \sigma] \qquad (a, b > 0) \tag{27}$$

and we have a slow, logarithmic dependence of S_x^2 on σ ($\to 0$). The analogous result for the three-dimensional case is:

$$\Delta_H^2 \simeq S_x^2 = n \times 0.1218\ldots,$$

as found long ago by Ronca and Allegra[26]. We see the interesting feature that the three-dimensional network has an unperturbed m.s size which, in the absence of any squeezing force, is comparable to that of a single chain strand. However, the energy vs. network size curve is infinitely steep in this case, so that further compression of this network requires the application of infinitely strong forces.

2. Polymer-mediated adhesion

2.1 The model

We are interested in modelling adhesion phenomena produced by a thin layer of polymer chains confined between two rigid parallel walls.

Our aim is to derive the small-strain tangential and longitudinal moduli of the adhesive layer. We will not address its large-strain behaviour and ultimate failure properties, which are also very important for applicative purposes.

The chains are assumed to be very long, so that their unperturbed radii of gyration are much larger than the wall-to-wall distance L. As a matter of fact, we consider a single infinitely long chain, compressed by the walls to melt-like densities (see Figure 2). We assume that, at a given instant in time, all the chain monomers in contact with the walls react and form permanent chemical bonds with it. The original infinite chain is thus broken up into shorter subchains, with their two end monomers either on the same or on opposite surfaces ("loops" and "bridges", respectively). The distribution of lengths for the loops and bridges, as well as their relative probabilities, is not given a priori, but will be derived from statistical principles. Thus, formation of irreversible polymer-surface bonds corresponds to taking an "instantaneous snapshot" of an equilibrium configuration the system — an idea pioneered some time ago by Deam and Edwards in the context of polymer networks [27]. Unlike the previous section, now there are no cross-links between the chain(s). Note that the present system corresponds to the "Model B" of ref. [13]. In the same paper, we also investigated the properties of a so-called "Model A", consisting of monodisperse polymer chains bridging the two surfaces.

We adopt a lattice model, following earlier treatments by Di Marzio [31], Scheutjens and Fleer[32], Silberberg [33] and one of us[34]. The statistical segments of the polymer lie on the edges of cubic cells. The lattice model is in many ways artificial, but it has also some distinct advantages. In particular, it allows the enumeration of the chain conformations and we implement it in a way which accounts exactly for finite chain extensibility (unlike Gaussian models). The more realistic representation of the interaction with a solid wall, compared with the harmonic potential of the previous section, is an additional bonus. The polymer is assumed to be in a rubbery amorphous state above its glass transition temperature, with a perfectly uniform density across the slab. The latter constraint is implemented by application of a suitable short-range polymer-wall attractive potential.

2.2 The transfer matrix

We consider two walls at a distance L, in cubic lattice units (equal to the length of the chain segments). Thus, L is also the number of lattice "layers" between the bottom and the top wall. We denote by $\mathbf{P}_L$ the

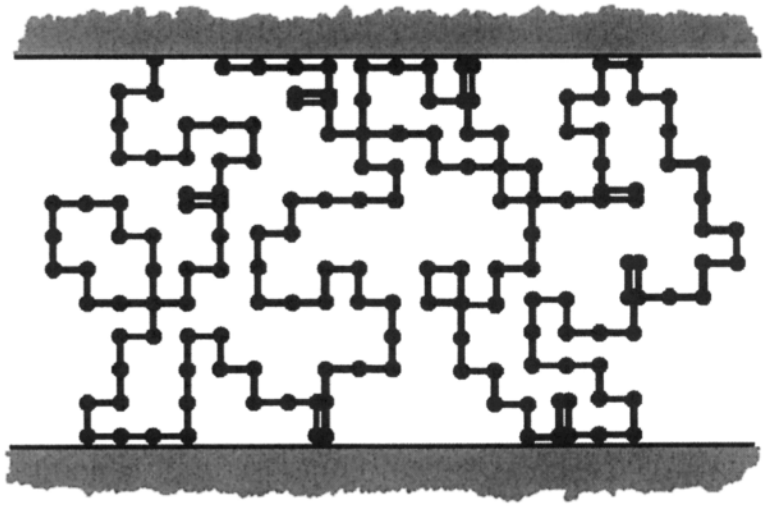

Figure 2. Representation of a very long chain filling the space between two parallel walls, forming loops, bridges and trains of variable length. The slab width is in this case $L = 12$. All the beads in contact with a wall are irreversibly bonded to it, after reaching configurational equilibrium.

$L \times L$ transfer matrix:

$$\mathbf{P}_L = \begin{bmatrix} 4 & 1 & 0 & 0 & \dots & 0 \\ 1 & 4 & 1 & 0 & \dots & 0 \\ 0 & 1 & 4 & 1 & \dots & 0 \\ \dots & \dots & \dots & \dots & \dots & \dots \\ 0 & \dots & 0 & 1 & 4 & 1 \\ 0 & \dots & 0 & 0 & 1 & 4 \end{bmatrix} . \tag{28}$$

Its (i, j) element represents the number of ways of placing one bond on the lattice, so as to connect a bead on layer i with a bead on layer j. Its eigenvalues λ_k and eigenvectors $\mathbf{a}_k = [a_{1k}, a_{2k}, \dots, a_{Lk}]$ are:

$$\lambda_k = 4 + 2\cos\left(\frac{\pi k}{L+1}\right), \tag{29}$$

$$a_{hk} = \sqrt{\frac{2}{L+1}} \sin\left(\frac{\pi hk}{L+1}\right). \tag{30}$$

We illustrate the usage of the transfer matrix by writing the partition functions — equal to the total number of allowed conformations, since there are no energetic terms associated with chain bending or bead-bead

interactions — of a chain of n segments, whose ends are constrained to lie either on the same ("loop", LP) or on opposite walls ("bridge", BR). In the first case we have:

$$Z_{\mathrm{LP}}(n,L) = \left[\begin{array}{ccccc} 1 & 0 & 0 & \cdots & 0 \end{array}\right] \mathbf{P}_L^n \left[\begin{array}{c} 1 \\ 0 \\ 0 \\ \vdots \\ 0 \end{array}\right] = \sum_{k=1}^{L} a_{1k}^2 \lambda_k^n, \qquad (31)$$

whereas in the second case:

$$Z_{\mathrm{BR}}(n,L) = \left[\begin{array}{ccccc} 1 & 0 & 0 & \cdots & 0 \end{array}\right] \mathbf{P}_L^n \left[\begin{array}{c} 0 \\ 0 \\ 0 \\ \vdots \\ 1 \end{array}\right] = \sum_{k=1}^{L} (-1)^{k-1} a_{1k}^2 \lambda_k^n. \qquad (32)$$

2.3 Statistical population of loops and bridges

As mentioned above, we consider a infinitely long chain, which is initially unconstrained and free to reach statistical equilibrium. The chain meanders between the walls, forming loops and bridges *of all possible lengths* n. We label their partition functions by $\bar{Z}_{\mathrm{LP}}$ and $\bar{Z}_{\mathrm{BR}}$. These differ from the partition functions of the previous section since:

a. In the present context, a bridge/loop presesents a chain travelling from one to the other/same surface, *without ever touching either wall* in the intermediate steps (otherwise, the chain would be further broken down into shorter bridges and/or loops).

b. We wish to model a situation with a uniform polymer density across the wall-to-wall slab. However, a phantom chain interacting with purely repulsive walls would have a density maximum at the middle, since it suffers from "entropic repulsion"[15, 34]. This is understood by recognizing that, on a simple cubic lattice, a segment within the bulk has six possible orientations. Instead, when one of its end beads is in contact with a wall, the segment has only five possible orientations. This can be remedied by placing a suitable "premium" on the monomers which are directly in contact with a wall.

In practice, the above requirements are implemented in the following way:

i. The two terminal bonds are constrained to be orthogonal to the surface, so that the effective number of *free* bonds in a subchain of n segments is $n-2$.

ii. We use a matrix $\mathbf{P}$ of order $L-2$ instead of L as in Eq.(28), to fordid the internal beads from visiting the upper and lower layer.

iii. The premium for the atoms at either wall is obtained by multiplying the partition function of each subchain by a factor of $\frac{6}{5}$. There is only one such factor, even though each subchain has two terminal beads, to avoid double counting of the chain-wall contacts.

These points may be summarized as:

$$\bar{Z}_{\mathrm{X}}(n,L) = \frac{6}{5} Z_{\mathrm{X}}(n-2, L-2) \quad (n, L \geq 2;\ \mathrm{X} = \mathrm{LP\ or\ BR}). \tag{33}$$

Finally, one should not forget that the chain may also form "trains" of segments in contact with the walls (see again Figure 2). These will be dealt with implicitly, since a train may be viewed as a sequence of "one-segment loops". All that is required is the additional rule:

iv. A one-segment loop (a chain bond lying flat on a wall) has the partition funtion:

$$\bar{Z}_{\mathrm{LP}}(1,L) = \frac{24}{5}, \qquad (\forall\, L) \tag{34}$$

given by the $\frac{6}{5}$ premium times the number of possible orientations of the segment (four).

The relative populations of loops and bridges are expressed by their probabilities:

$$p_{\mathrm{X}}(n,L) = \frac{\bar{Z}_{\mathrm{X}}(n,L)}{6^n}, \tag{35}$$

where 6^n is the partition function of a generic *unconstrained* n-segment section of an infinitely long chain. It ensures the fulfilment of the normalization condition:

$$\sum_{n=1}^{\infty} [p_{\mathrm{LP}}(n,L) + p_{\mathrm{BR}}(n,L)] = 1. \tag{36}$$

These quantities are given graphically in Figures 3 and 4, for some selected strand lengths or slab widths. We observe that, for a given strand length, the loop and bridge probabilities are virtually identical up to wall-to-wall distances of the order of the unperburbed radius of gyration, i.e. up to $L \simeq \sqrt{n}$. Afterwards, the loop probability tends to

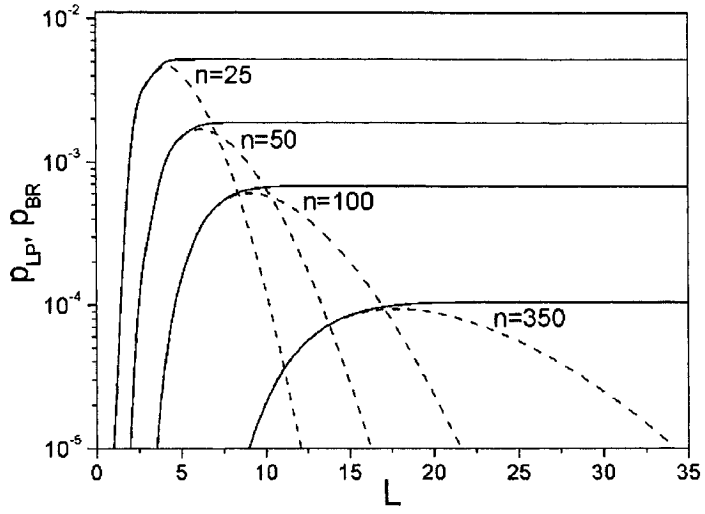

Figure 3. Probabilities of loops (solid lines) and bridges (dashed lines) of selected lengths n, as a function of the wall-to-wall distance L.

a constant value, whereas the bridge probability drops to zero. Short loops are always more more likely to occur than long ones. Instead we observe a crossover for bridges, since a short bridge is more probable than a long one for narrow slits, and less probable for wider slits. For a given wall-to-wall distance L, the most probable bridges have a strand length $n \simeq L^2$.

The average strand length is defined as

$$\langle n \rangle = \sum_{n=1}^{\infty} n \left[p_{\mathrm{LP}}(n, L) + p_{\mathrm{BR}}(n, L) \right] . \tag{37}$$

It has a simple expression, which may be obtained by the following argument. We know from ref.[34] that, if the density on the internal layers is equal to ρ, the density on the terminal ones is $\frac{5}{6}\rho$. The total number of beads within the slab is thus:

$$N = \rho S \left[(L-2) + 2\frac{5}{6} \right] \tag{38}$$

where S is the slab area ($\to \infty$). Since the infinite superchain is broken into two separate strands whenever one of its beads touches one of the

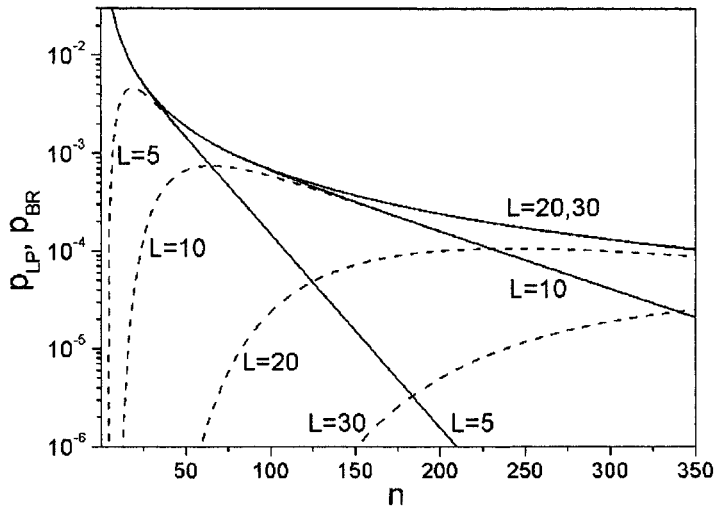

Figure 4. Probabilities of loops (solid lines) and bridges (dashed lines) for some selected wall-to-wall distances L, as a function of their length n.

walls, we may obtain $\langle n \rangle$ from the ratio of the total number of beads and the number of beads on the terminal layers:

$$\langle n \rangle = \frac{N}{2\frac{5}{6}\rho S} = \frac{3}{5}L - \frac{1}{5}. \tag{39}$$

The average strand length is nearly proportional to the slab width. It is actually smaller than it, since loops are always more probable than bridges (for a given strand length).

2.4 Free energy, elastic forces and moduli

The Helmholtz free energy of a single chain strand may be evaluated according to the usual statistical-mechanical recipe $A_{\mathrm{X}}(n, L) = -\ln \bar{Z}_{\mathrm{X}}(n, L)$ (where X=LP or BR). On the other hand, the free energy of an ensemble of chains whose terminals are irreversibly bonded to the walls is obtained by averaging the free energies of the strands, weighting them by the loop and bridge probabilities calculated in the previous section:

$$\mathcal{A}(L) = \sum_{n=1}^{\infty} \left[p_{\mathrm{LP}}(n, L_0) A_{\mathrm{LP}}(n, L) + p_{\mathrm{BR}}(n, L_0) A_{\mathrm{BR}}(n, L) \right]. \tag{40}$$

It is important to observe that the weighting coefficients are fixed at the time of the polymer-wall reaction(they are "quenched variables"). In general, they may correspond to the equilibrium configuration of the system at a slab width $L_0 \neq L$. Thus, the calculated properties are bound to depend on the "preparation conditions". There is a strong analogy with the elasticity of cross-linked rubbers, as discussed by Deam and Edwards[27].

The elastic forces are given by the first derivatives of the free energy $\mathcal{A}(L)$ with respect to diplacements of the two walls, referred to a unit surface. Since the loop and bridge probabilities are constant, all that is required are the derivatives of A_{LP} and A_{BR} for all possible strand lengths. The evaluation of normal (logitudinal) forces is in principle straightforward:

$$f_{\mathrm{X}}(n,L) = \frac{\partial A_{\mathrm{X}}(n,L)}{\partial L} = -\frac{1}{\bar{Z}_{\mathrm{X}}(n,L)} \frac{\partial \bar{Z}_{\mathrm{X}}(n,L)}{\partial L}. \tag{41}$$

According to our sign convention, f_{X} is positive for attractive wall-wall forces (i.e., adhesion) and negative for repulsive ones. We computed these derivatives by numerical differentiation, using quadruple precision arithmetic (necessary for accurate summation of Eqs.(31) and (32)). The result is as expected on simple physical grounds. Loops and bridges exert virtually identical repulsive forces up to $L \simeq n$ (the unperturbed strand size). At larger distances, the loop forces vanish, whereas the bridge forces turn into attractive. They are linear at moderate extensions, and they take the inverse Langevin form [35] as the chain approaches its maximum elongation.

Since we are neglecting entanglement effects, only the strands which bridge the two walls contribute to shear (tangential) forces. Evaluation of these forces is slightly more complicated, but luckily the results may be summarized in a very simple and concise way. In the limit of small lateral displacements σ, the force is linear and given by:

$$f_{\mathrm{BR}}(n,L,\sigma) = \frac{2\sigma}{n_{||}}. \tag{42}$$

Here $n_{||}$ is the average number of bonds parallel to the surfaces, which is in turn given by:

$$n_{||} = 4n \frac{\bar{Z}_{\mathrm{BR}}(n-1,L)}{\bar{Z}_{\mathrm{BR}}(n,L)}. \tag{43}$$

The elastic moduli κ_{long} and κ_{tan} are obtained by further differentiation of the forces per unit area (they are second derivatives of the free energy). We skip the mathematics and go directly to the final results in

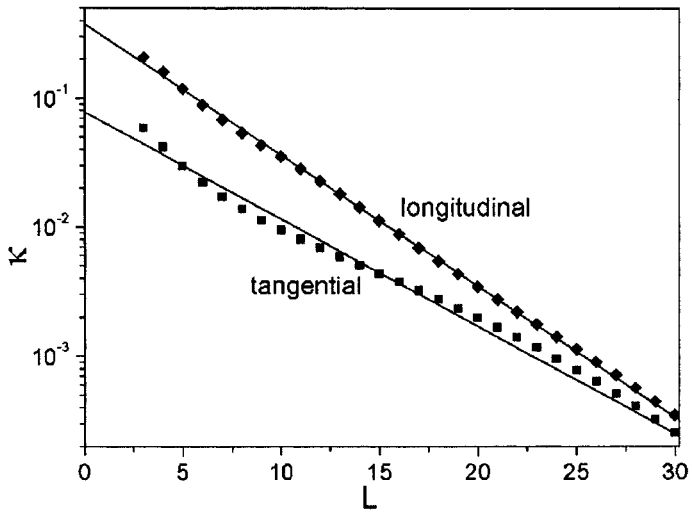

Figure 5. Tangential and longitudinal moduli, as a function of the wall-to-wall distance L. The symbols represent the computed points, the straigth lines are least-square fits.

Figure 5. The plots give the two moduli as a function of the wall-to-wall separation. They have been obtained for $L = L_0$, at wall-to-wall distances identical to those at cross-linking [see eq.(40)]. The longitudinal modulus is roughly one order of magnitude larger than the tangential one at small L's. Both moduli decay to zero in a roughly exponential way at larger L's:

$$\kappa(L) = \bar{\kappa}\, 10^{-L/\bar{L}}. \tag{44}$$

Fits of the log-linear plots within the range $4 \leq L \leq 30$ give:

$$\bar{\kappa}_{\text{long}} = 0.376\,, \qquad \bar{L}_{\text{long}} = 9.86\,;$$
$$\bar{\kappa}_{\text{tan}} = 0.078\,, \qquad \bar{L}_{\text{tan}} = 12.0\,.$$

The basic reason for the fast decay of the force constants with inceasing thickness is that fewer and fewer short chains connect the two walls (see again Figs. 3 and 4), whereas the long chains contribute much less to the modulus. It should also be borne in mind that, in the absence of the walls and of a polymer-surface reaction, the polymer would be a simple rubbery liquid with a null zero-frequency shear modulus.

As a final note of caution, we point out that the conformational entropy of the chains is only one of the contributions to the elastic modulus. In particular, under extension the polymer layer must undergo substantial volume changes (instead, there is roughly no volume change for shear deformations). This may be associated with important enthalpic effects, whose contribution to the elongational modulus may be estimated by a Flory-Huggins energetic term incorporating a suitable χ parameter[14, 15, 28]. Once more, see ref. [13] for details.

3. Conclusions

We have summarized two recent theoretical papers on the elasticity of polymer networks and chains confined within narrow slits[12, 13]. The neglect of polymer-polymer interactions (phantom chain assumption) allows an essentially exact — although sometimes complicated — mathematical description. The presentation has been didactic in spirit and we have strived to highlight the essential physics of these systems. Hopefully this will stimulate more theoretical, experimental and computational studies.

The problem of polymer-mediated adhesion would certainly deserve further scrutiny. We are not aware of any experimental or computational studies of systems directly related to our model (very long chains, irreversibly bonded to both surfaces of two confining walls). All the experimental work by the surface force apparatus [1, 5–10] has concentrated on confined polymer melts and solutions or interpenetrating polymer brushes (chains bonded at one end only). Presumably, one of the reasons for this is that irreversible chemical bonding at both surfaces is not easily reconciled with reversible and easily repeatable experiments (at the end of each experiment, a large extensional force would have to be applied, in order to break the polymer film and bring the surfaces apart). It may be possible to circumvert this problem by exploiting easily hydrolizable polymer-surface bonds, such as those of the ester or amide functional groups. Computer experiments are also expected to provide important qualitative insights and quantitative results. The simulation of irreversible chemical bonding at the polymer-wall interface and of the mechanical properties of the resulting adhesive films may be expected to be very challenging steps, in analogy with computer simulations of chemically cross-linked networks[36, 37].

Acknowledgments

We thank Paolo Pasini and Claudio Zannoni for inviting us to contribute this paper. We have benefited from the financial support of the Italian MIUR through COFIN2003.

References

[1] J. Israelachvili, *Intermolecular and Surface Forces*, 2nd ed., Academic Press, London, 1994.

[2] S. Granick (editor), *Polymers in Confined Environments*, *Adv. Polym. Sci.*, 138, Springer, Berlin, 1999.

[3] R.G. Larson, *The Structure and Rheology of Complex Fluids*, Oxford University Press, Oxford, 1999.

[4] A.V. Pocius, *Adhesion and Adhesives Technology, An Introduction*, Hanser Publishers, Munich Vienna and New York, 1997.

[5] P.F. Luckham and S. Manimaaran, *Adv. Colloid Interf. Sci.*, 73:1 1997.

[6] G. Luengo, F.-J. Schmitt, R. Hill and J. Israelachvili, *Macromolecules*, 30:2482, 1997.

[7] M. Ruths and S. Granick, *J. Phys. Chem. B*, 103:8711, 1999.

[8] H.S. Kim, W. Lau and E. Kumacheva, *Macromolecules*, 33:4561, 2000.

[9] U. Raviv, R. Tadmor and J. Klein, *J. Phys. Chem. B*, 105:8125, 2001.

[10] S. Yamada, G. Nakamura and T. Amiya, *Langmuir*, 17:1693, 2001.

[11] P.A. Schorr, T.C.B. Kwan, S.M. Kilbey II, E.S.G. Shaqfeh and M. Tirrel, *Macromolecules*, 36:389, 2003.

[12] G. Allegra and G. Raos, *J. Chem. Phys.*, 116:3109, 2002.

[13] G. Allegra, G. Raos and C. Manassero, *J. Chem. Phys.* 119:9295, 2003.

[14] P.-G. de Gennes, *Scaling Concepts in Polymer Physics*, Cornell University Press, Ithaca, 1985.

[15] A.Yu. Grosberg, A.R. Khokhlov, *Statistical Physics of Macromolecules*, American Institute of Physics, NewYork, 1994.

[16] D.Y. Yoon, M. Vacatello and G.D. Smith, in *Monte Carlo and Molecular Dynamics Simulations in Polymer Science*, K. Binder ed., ch. 8, p. 433, Oxford University Press, New York, 1995.

[17] M. Vacatello, *Macromol. Theory Simul.*, 11:53, 2002.

[18] A. Milchev and K. Binder, *Eur. Phys. J. B*, 3:477, 1998.

[19] C. Mischler, J. Baschnagel and K. Binder, *Adv. Colloid Interf. Sci.*, 94:197, 2001.

[20] A. Alexander-Katz, A.G. Moreira and G.H. Fredrickson, *J. Chem. Phys.*, 118:9030, 2003.

[21] T. Aoyagi, J. Takimoto and M. Doi, *J. Chem. Phys.*, 115:552, 2001.

[22] A. Yethiraj, *Adv. Chem. Phys.*, 121:89, 2002.

[23] T. Kreer, M.H. Müser, K. Binder and J. Klein, *Langmuir*, 17:7804, 2001.

[24] B. Park, M. Chandross, M.J. Stevens and G.S. Grest, *Langmuir*, 19:9239, 2003.

[25] H.M. James and E. Guth, *J. Chem. Phys.* 10: 455, 1943; H.M. James, *J. Chem. Phys.* 15:651 1947.

[26] G. Ronca and G. Allegra, *J. Chem. Phys.*, 63:4104, 1975.

[27] R.T. Deam and S.F. Edwards, *Philos. Trans. R. Soc. London, Ser. A*, 280:317, 1976.

[28] B. Erman and J.E. Mark, *Structure and Properties of Rubberlike Networks*, Oxford University Press, New York and London, 1997.

[29] P.E. Rouse, *J. Chem. Phys.*, 21:1272, 1953.

[30] M. Doi and S.F. Edwards, *The Theory of Polymer Dynamics*, Clarendon Press, Oxford, 1986.

[31] E.A. Di Marzio, *J. Chem. Phys.*, 42:2101, 1965; E.A. Di Marzio and R.J. Rubin, *J. Chem. Phys.*, 55:4318, 1971.

[32] J.M.H.M. Scheutjens and G.J. Fleer, *J. Phys. Chem.*, 83:1619, 1979; *ibid.*, 84:178, 1980.

[33] A. Silberberg, *J. Coll. Interf. Sci.*, 90:86, 1982.

[34] G. Allegra and E. Colombo, *J. Chem. Phys.*, 98:7398, 1993.

[35] P.J. Flory, *Statistical Mechanics of Chain Molecules*, Hanser, NewYork, 1989.

[36] K. Kremer and G.S. Grest, in *Monte Carlo and Molecular Dynamics Simulations in Polymer Science*, K. Binder ed., ch. 4, p. 194, Oxford University Press, New York, 1995.

[37] F.A. Escobedo and J.J. de Pablo, *Phys. Rep.*, 318:85, 1999.